Design of Isolated DC Solar Powered Microgrid with Storage System

Zeina Bahij[1], Abdulla Ismail[2]

[1]Graduate Student, Dept. of Electrical Engineering, Rochester Institute of Technology, Dubai, UAE
[2]Professor, Dept. of Electrical Engineering, Rochester Institute of Technology, Dubai, UAE

Abstract - *The use of green energy has been of wide interest in recent decades it limits emissions and produce cheap energy due to the fact that they depend on renewable energy resources that are available at no cost. However, these resources are intermittent and can not stand alone to support a Microgrid system to satisfy the demand. This can be solved by using an energy storage system. In this paper, an electrical model of the photovoltaic system is presented. Parameters from datasheet of a photovoltaic system, I(V) and P(V) characteristics plot are used to calculate the exact series and shunt resistances. The variable output power of the PV system was controlled by Boost converter that uses MPPT algorithm. Energy system used in this paper is the battery energy storage system (BESS) based on Lithium ion batteries controlled by Buck-Boost converter that uses PID controller.*

Key Words: Microgrid, Photovoltaic System, Battery Energy Storage System.

I. INTRODUCTION

1.1 Photovoltaic Cell

Photovoltaic cell is a device that is used to convert sunlight energy into power. It is becoming of wide interest worldwide since it uses a renewable energy resource to produce green energy that will reduce emissions.

Solar cells consist of a p-n junction fabricated in a thin wafer or layer of semiconductor. In the dark, the I-V output characteristic of a solar cell has an exponential characteristic similar to that of a diode.

When exposed to light, photons with energy greater than the bandgap energy of the semiconductor are absorbed and create an electron-hole pair. These carriers are swept apart under the influence of the internal electric fields of the p-n junction and create a current proportional to the incident radiation. When the cell is short circuited, this current flows in the external circuit; when open circuited, this current is shunted internally by the intrinsic p-n junction diode. The characteristics of this diode therefore sets the open circuit voltage characteristics of the cell. [1]

The performance of a solar cell can be demonstrated by measuring its current versus the voltage. The IV curve is the superposition of the IV curve of the solar

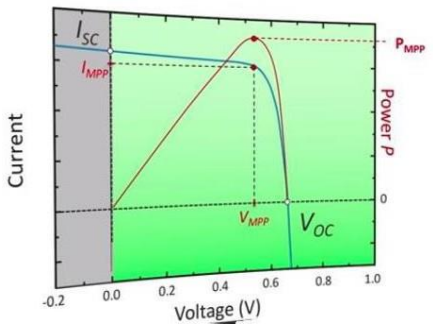

Figure 1 IV and PV characteristics of PV [2]

cell diode in the dark with the light-generated current. Both parameters, VOC and ISC, define the IV curve. The power of a solar cell is defined as the voltage multiplied by the current at any point on the IV curve. With the IV curve it is possible to determine the maximum power point (MPPT). In Figure 1, it is represented the power versus the current (red line). The current and voltage where the maximum power point is located are also two parameters that define the characteristics of the solar module. That power is the one delivered to the rest of the PV system and eventually to the load. Therefore, it is essential that the solar module operates at the maximum power. [2]

The simplest equivalent circuit of a solar cell is a current source connected in anti-parallel way with a light current source [3]. This model does not take into account the internal losses of the current. Figure 2 shows the equivalent circuit.

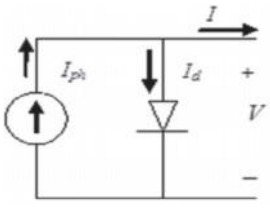

Figure 2 Simplest Equivalent Circuit of Solar Cell [3]

Using Kirchhoff law to calculate the output current:

$$I = Iph - Id \quad (1)$$

where Iph is the photocurrent.

Id is the diode current given by

$$I_d = I_0 \left[\exp\left(\frac{V}{N_s V_T}\right) - 1\right]$$
(2)

where V is the voltage imposed on the diode.

V_T is the Thermal Voltage

$$V_T = k\, T_c / q \qquad (3)$$

I_0 is the leakage current of the diode (A) Tcis the actual cell temperature (K).

K is the Boltzman constant (1.381 x 10^{-23} J/K) qis the electron charge (1.602 x 10^{-19} C)

N_s is the number of PV cells connected in series and A is the the ideality factor depends on PV Technology.

In real life, it is impossible to neglect current losses, so series resistance Rs and Parallel resistance Rp are added to the circuit. Series resistances are caused by the contact resistance between the metal contact and the silicon, the movement of current through the emitter and the base of the solar cell and the resistance of the top and rear metal contacts. While shunt resistance causes significant power losses typically due to manufacturing defects rather than poor solar cell design. Figure 3 shows the real circuit of a solar cell.

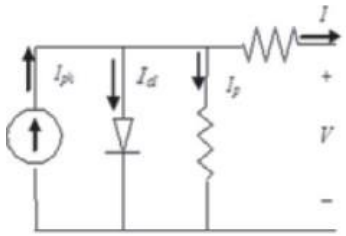

Figure 3 Real Life Equivalent Circuit of Solar Cell [3]

Adding series resistor will lead the revised Id as:

$$I_d = I_0 \left[\exp\left(\frac{V+IR_S}{a}\right) - 1\right]$$
(4)

where a is the thermal voltage given as

$$a = \frac{N_S\, A\, k\, T_C}{q} = N_S A\, V_T$$
(5)

By applying Kirchhoff law to circuit in figure 2, output current will be

$$I = I_{ph} - I_d - I_p$$
(6)

where I_p is the current across Rp

The output current then is given as

$$I = I_{ph} - I_0 \left[\exp\left(\frac{V+IR_S}{a}\right) - 1\right] - \frac{V+IR_S}{R_P}$$
(7)

where $I_{ph} = \frac{G}{100}[I_{SCR} + K_I(T - 25)]$
(8)

and $I_O = I_{or}\left(\frac{T}{T_r}\right)^3 \exp[\frac{qE_{GO}}{BK}(\frac{1}{T_r} - \frac{1}{T})]$
(9)

where I_{sc} is the short circuit current.

A. *Battery Storage System*

Energy Storage Systems (ESS) have been used in conventional power systems for some time. With the wide use of smart grids, ESS are becoming of more importance due to the use of renewable energy resources which can not satisfy the load demand at all times due to their intermittency nature. Hence, energy from these resources must be stored when the generated power exceeds the power demand, so it can be used later to satisfy load demand. ESS are of many types, compressed air, super capacitor, flywheel, pump storage and batteries. Selection of the suitable battery energy storage system depends on many factors including capacity, performance and cost. The most commonly used energy storage system is the battery energy storage system (BEES) [4]. Batteries can convert electrical energy into chemical energy while charging, and convert back into electrical energy while discharging.

The rechargeable batteries have been enhanced from lead acid to nickel-based battery and then to lithium ion batteries. Lithium-ion battery is a relatively new technology that was first commercialized in 1991[5]. Lithium-ion batteries are known to their following advantages:

1. High energy density: large scale ESS require the use of specific energy and energy density [6]. At early stages, Li-ion battery were of energy density of order 200 Wh/L. In 2012, energy density was enhanced to reach order of 725 Wh/L. [7]
2. Long life time: Current Li-ion technology under test in-grid connected system is used. It has a lifetime of 20 years at 60% depth of discharge (DOD) per day. At 100% degree of discharge the battery can operate over 6000 cycles.
3. High Efficiency: 94% efficient over 100% Degree of discharge. Efficiencies of 98% have been found for small discharges in case the battery is close to full charge. 91% is the maximum efficiency drop owing to cells' age, which is much more efficient compared to other technologies. [8][9]

The disadvantages of Li-ion batteries are:
1. Lifetime will be shortened in case it was completely discharged.
2. Discharging a battery with high currents cause damage.
These disadvantages are commonly avoided by using electronic circuits for management of charging and discharging processes of the battery.

2. MODELING

2.1 PV System Modeling

In order to find the best model, several parameters have to be calculated. In [10], a model of moderate complexity was used where the temperature dependence of the photo-current IL, saturation current of the diode I_0., series resistance R_S were included, but effect of the shunt resistance was neglected.

The equations to describe the IV characteristics where as follows:

Photo current: $I_L = G\frac{I_{SC(T1)}}{G_0}[\,1+K_0(T-T_1)]$ *(10)*

Where $K_0 = \frac{I_{SC(T2)}-I_{SC(T1)}}{T_2-T_1}$ *(11)*

$$I_O = I_{d0}\left(\frac{T}{T_r}\right)^{3/n}\exp[-\frac{q}{nK}V_g(\frac{1}{T_r}-\frac{1}{T})] \quad (12)$$

$$I_{d0} = \frac{I_{SC(T1)}}{\exp(\frac{qV_{OC(T1)}}{T1}-1)} \quad (13)$$

In [11] Iph, I_0, R_S, R_P were calculated. Photocurrent is calculated assuming that when PV model is short-circuited, $I_{ph} = I_{SCRef}$, which is the short circuit current reference, calculated at the standard test conditions (STC). So, the photocurrent:

$$I_{ph} = \frac{G}{G_{ref}}(I_{ph,ref} + \mu_{sc}\Delta T) \quad (14)$$

where G is the Irradiance (W/m2)

Gref is the Irradiance at STC= 1000 W/m2

ΔT =Tc - Tc,ref (Kelvin) *(15)*

$T_{c,ref}$ is the Cell temperature at STC = 25+ 273 =298 K,

μ_{SC} is the Coefficient temperature of short circuit current (A/K), provided by the manufacturer

$I_{ph,ref}$ is the Photocurrent (A) at STC.

At the end of that study Rs= 0.45 Ω and Rp= 310.0248 Ω.

Taking the most remarkable points at standard test condition: the voltage at open circuit (I =0, V= $V_{oc,ref}$), the current at short circuit (V =0, I= $I_{sc,ref}$), and the voltage ($V_{mp,ref}$) and current ($I_{mp,ref}$) at maximum power, the reverse saturation current is:

$$I_0 = I_{SCref}\exp(\frac{V_{oc,ref}}{a}\left(\frac{T_c}{T_{c,ref}}\right)^3\exp[(\frac{q\varepsilon_G}{AK})(\frac{1}{T_{c,ref}}-\frac{1}{T_C})] \quad (16)$$

Series and shunt resistors are calculated at maximum power point, Rs is first set to zero and then slowly increased until experimental and theoretical MPP are equal, then Rp is calculated using the following:

$$R_p = \frac{V_{mp,ref}+I_{mp,ref}R_s}{I_{sc,ref}-I_{sc,ref}\{\exp[\frac{V_{mp,ref}+I_{mp,ref}R_s-V_{oc,ref}}{a}]\}+I_{sc,ref}\{\exp\left(-\frac{V_{oc,ref}}{a}\right]\}-\frac{P_{ma}}{V_{mp}}} \quad (17)$$

In this work, parameters to be evaluated will be the series and shunt resistances. First, equations of photocurrent and the saturation current of the diode from [11], which does not consider shunt resistance, were used to plot the IV and PV characteristics. Then, series resistance will be incremented from 0 till the maximum power point is achieved at the maximum voltage at STC referring to Table 1. Shunt resistance is then calculated using equation (17).

Table 1 Parameters of PV at STC

Parameters	Values
Maximum Power Point P_{mp} (W)	49
Maximum Current Point I_{mp} (A)	2.88
Maximum Voltage Point V_{mp} (V)	17
Short Circuit Current I_{sc} (A)	3.11
Open Circuit Voltage V_{oc} (A)	21.8
Series Resistance R_s (Ω)	0.55
N_{oct} (^{0}C)	45
Coefficient temperature μ_{sc} (K^0)	1.3 x 10

K_d	-72.5 x 10
Cells Connected in Series N_s	36

2.2 Modeling of the Battery System

Figure 4 shows the equivalent circuit of the battery Model implemented in Matlab. It contains the internal resistance and the voltage controlled source. This voltage source is controlled by the charging and discharging voltages which depend on the battery type.

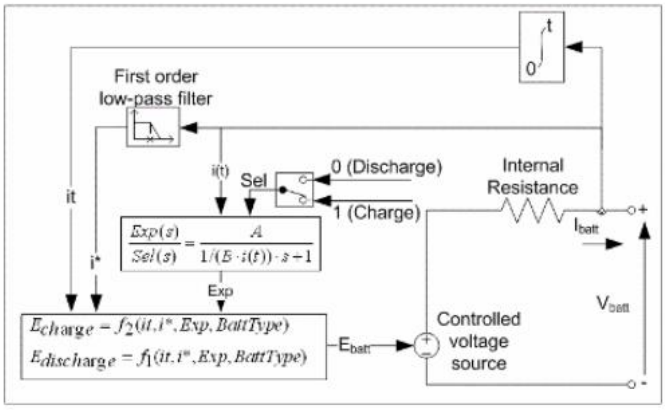

Figure 4 Battery Model in Matlab [12]

For Lithium ion battery the mathematical models are as follows: [12]

- Discharge Model (i* > 0)

$$f1\,(it, i*, i) = E_0 - K\frac{Q}{Q-it}i* - K\frac{Q}{Q-it}it + A\exp(-B.it) \quad (18)$$

- Charge Model (i* > 0)

$$f2\,(it, i*, i) = E_0 - K\frac{Q}{0.1Q+it}i* - K\frac{Q}{Q-it}it + A\exp(-B.it) \quad (19)$$

where

- E_{Batt}: nonlinear voltage, in V.
- E_0: constant voltage, in V.
- *Exp(s)*:exponential zone dynamics, in V.
- *Sel(s)* represents the battery mode.

  Sel(s) = 0 during battery discharge, *Sel(s)* = 1 during battery charging.
- *it*: extracted capacity, in Ah.
- *K*: polarization constant, in V/Ah, or polarization resistance, in Ohms.
- *i**: low-frequency current dynamics, in A.
- *i*: battery current, in A.
- *Q*: maximum battery capacity, in Ah.
- *A*: the exponential voltage, in V.
- *B*: the exponential capacity, in Ah^{-1}.

A single battery of fully charged voltage of 4.2 V is not enough for a Microgrid modeling. Several batteries must be connected to increase capacity, nominal voltage, fully charged voltage and nominal discharge current. Parameters of single Lithium battery were extracted from the datasheet and are shown in Table 2.For connected batteries, parameters will be as shown in Table 3.

Panasonic Lithium-Ion CGR18650AF Lithium Ion Battery is used. 36 batteries are connected in series and 125 batteries are connected in parallel here for a rated capacity of 800 Ah and the nominal voltage will be 130 V. BESS was summed to have initial charge of 100%. Temperature effects are neglected in this study, since the difference between maximum and minimum temperature used in the PV model in section 3.3 is 9^0.

Table 2 Extracted Parameters of the Panasonic Lithium-Ion CGR18650AF

Parameter	Value
Nominal Voltage (c)	3.3 V
Rated Capacity	2.05 Ah
Maximum Capacity (d)	2 Ah
Fully Charged Voltage (a)	4.2 V
Nominal Discharge current	1.95 A
Internal resistance (estimated)	16.5 mΩ
Capacity at nominal voltage (c)	1.81 Ah
Exponential zone (b)	[3.71 V, 0.6 Ah]
Nominal ambient temperature	25^0C
Second ambient temperature	0^0C
Maximum capacity at 0^0C (h)	1.78 Ah
Initial discharge voltage at 0^0C (e)	4 V
Voltage at 90% maximu capacity at 0^0C (g)	3.11 V
Exponential Zone at 0^0C (f)	[3.8 V, 0.2 Ah]
Thermal resistance, cell-to-ambient (estimated)	0.06
Thermal time constant, cell-to-ambient (estimated)	1000

Table 3 Parameters of Connected Batteries

Parameter	Value
Nominal Voltage	1.18 *Nb_ser
Rated Capacity	6.5 *Nb_par
Maximum Capacity	7 *Nb_par
Fully Charged Voltage	1.39 *Nb_ser
Nominal Discharge current	1.3 *Nb_par
Internal resistance (estimated)	0.002 Nb_ser/ Nb_par
Capacity at nominal voltage	6.25 *Nb_par
Exponential zone	1.18 *Nb_ser, 1.3 *Nb_par

3. CONTROL SYSTEMS

Converters are widely used to control the power flow, voltage, system balancing, maximum power point tracking and fault protection. [13] Converters switched mode power supplies, which can convert the DC voltage from one level to another. It can step up or step down the dc voltage source. Stepping up the voltage means stepping down the current and vice versa.

The dc-dc converters are widely used for traction motor control in electronic automobiles, trolley cars, marine hoists, forklift trucks, and mine haulers. They provide smooth acceleration control, high efficiency, and fast dynamic response. DC-DC converters can be used in regenerative braking of dc motors to return energy back into the supply, than this feature results in energy savings for transportation systems with frequent stops. [14] DC converters are used in dc voltage regulators and also are used in conjunction with an inductor, to generate a dc current source, especially for the current source inverter.

B. Control of PV Model

PV module produces variable power depending on irradiance and temperature and it reaches maximum power point, product of V_{mpp} and I_{mpp}, at specific irradiance and temperature. Maximum Power Point Tracking (MPPT) algorithm is used to extract maximum power from renewable energy resources like wind turbines and PV, under all conditions, since they produce variable power due to their intermittency nature [15][16]. Its main objective is to find the maximum power point and keep the load resistance, characterized by the I-V curve, at that point. MPPT devices are integrated into an electric power converter system that provides current or voltage conversion, regulation for driving various loads.

Many researchers has proposed different strategies to extract maximum power form PV using MPPT algorithm. In [17] tracking maximum power point using linear relationship between maximum voltage and open circuit voltage. In [18] the author used a look-up table to track techniques with measurement and comparison. The use of microcontrollers in power systems enables the implementation of AI techniques. In [19] Artifical Neural Network (ANN) MPPT controller was proposed based on fixed and variable step size, is proposed. In this work number of layers and neurons, parameters of training algorithim of the MPPT Controller were generated and then used in PV system.

Perturbation and Observation (P&O) technique is widely used. Its main advantage is that it is independent on PV generator characteristics, like solar intensity and cell temperature and can be implemented in analogue and digital circuits. It perturbs the operating point to let the voltage fluctuate around the maximum power point voltage despite the variation of irradiance and temperature[20]. This strategy is widely used because of its simplicity and efficiency. However, it lacks fast adaptability which is important to track fast transients under varying environment conditions[21-23]. In this research, incremental conductance MPPT is used. The IncCond method is the one which overrides over the aforementioned drawbacks. In this method, the array terminal voltage is always adjusted according to the MPP voltage. It is based on the incremental and instantaneous conductance of the PV module[24-27].

A boost converter of 5 kHz and 300 V reference is used to control the output of PV system, this boost converter is controlled by MPPT (incremental conductance + integral regulator).

Figure 5 shows the MPPT used for control of boost converter. Output voltage and current of the PV system are the inputs to the MPPT subsystem. A Deblock is used to switch MPPT on or off. MPPT subsystem is shown in Figure 6. Output of the MPPT

is the DC voltage reference subtracted from the Duty cycle and then used to generate pulses of the Pulse Width Modulation of frequency 5 kHz and initial value of 0.25. DC-DC converter is shown in Figure 7.

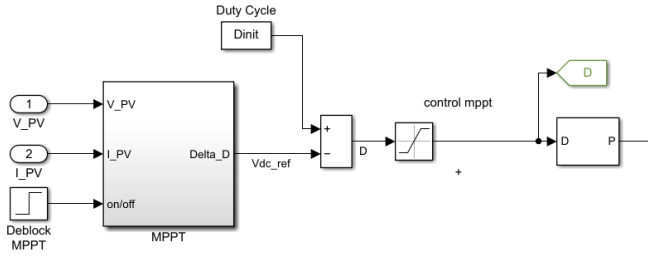

Figure 5 MPPT Boost Converter Control

Figure 6 shows the incremental conductance MPPT subsystem used. Its inputs are the output voltage and current of the PV system. The array terminal voltage is always adjusted according to the MPP voltage. It is based on the incremental and instantaneous conductance of the PV module.

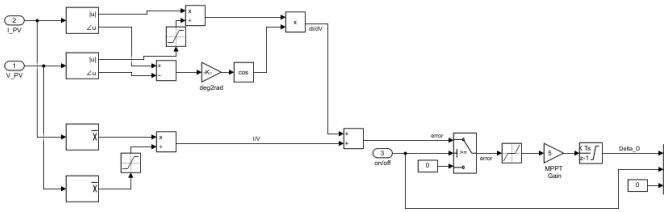

Figure 6 MPPT subsystem

Boost converter (Figure 7) boost the output voltage of the PV system to 300 V. When the switch is closed the inductor store energy and there is no current delivered the diode, energy will be supplied by the capacitor charge. Energy stored in the inductor will be delivered to the load to boost output voltage and recharge the capacitor when the switch is open. Inductor immediately reverse its electromagnetic field to opposes any drop in current. Voltage is controlled by varying the duty cycle that is pulses generated from the MPPT subsystem.

$$V_O = \frac{Vs}{1-D} \qquad (20)$$

Capacitor of capacitance 100 µF is used as a DC link. Resistor of resistance 0.005 Ω and inductor of inductance 5 mH was used.

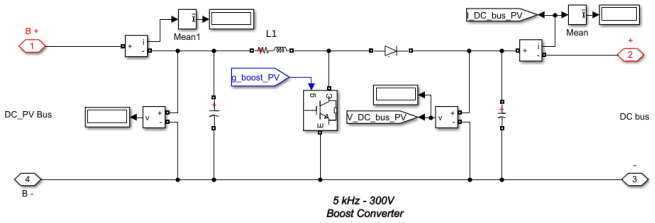

Figure 7 Boost Converter used to control PV system

C. *Control of Charging ad Discharging of the Battery System*

The buck boost converter operation is a combination of the buck and boost converter, it can lower or higher the output voltage according to the duty cycle, it is lower than 0.5 the output voltage will be less than the input voltage, else it will be more than the input voltage. Equation 21 shows the relation between duty cycle and output voltage.

$$V_O = \frac{-VsD}{1-D} \qquad (21)$$

Charging and discharging processes of the BESS is controlled using boost-buck converter as shown in Figure 8. A constant voltage at the DC bus is required 130 V is used as a voltage reference.

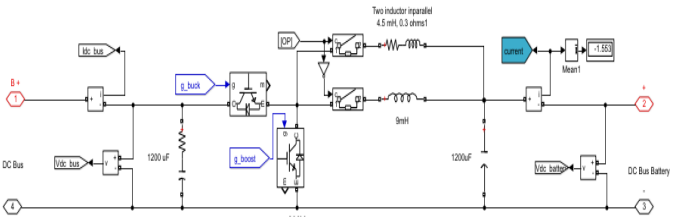

Figure 8 Boost-Buck Converter Used to Control BESS System

A capacitor of capacitance 12 µ6 and resistor of resistance 0.1 Ω is used as DC link. Two IGBT transistors are used one for controlling buck and the other for controlling the boost part. Inputs of the first switch are constants zero and 1, the switch output is the input of the breaker used for the buck-boost converter shown in Figure 9.

The voltage of the DC bus is compared with a reference voltage of 130 V (nominal voltage of the battery). If the voltage of the DC bus is greater than the reference voltage the battery will be charging, hence the boost converter will be activated. Otherwise, the battery will be discharged and the buck converter will be activated.

An error signal, which is the difference of the DC bus voltage and the voltage reference, is used for the PID controller. Figure 10 shows the PID Controller used with Ki= 3 and Kp=0.02 for the Boost voltage Controller. Figure 10 shows the PID Controller used with Ki= 110 and Kp=0.02 for the Buck voltage Controller.

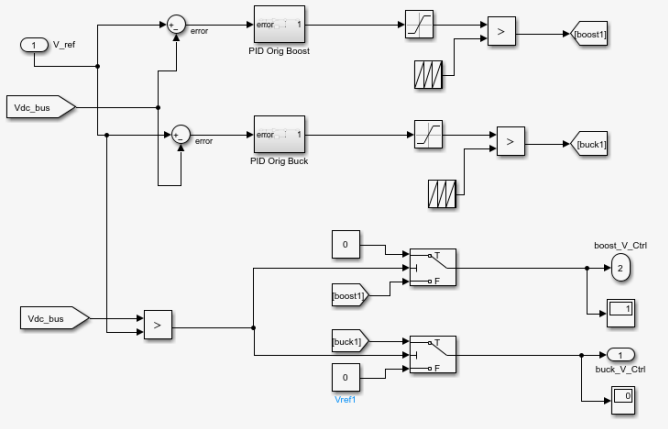

Figure 9 Voltage Controller of the Bidirectional Boost-Buck Converter

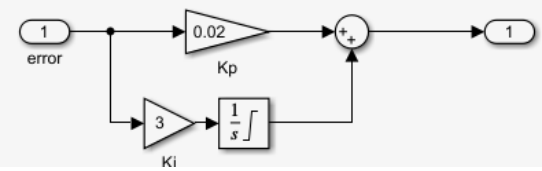

Figure 10 PID Controller for the Boost Voltage Controller

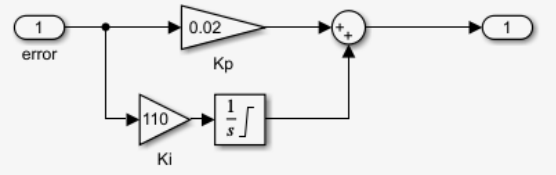

Figure 11 PID Controller for the Buck Voltage Controller

4. RESULTS

4.1 Results of the PV Model

Figure 12 shows the IV characteristics in Rs model without considering shunt resistance. As series resistance increases, maximum voltage point decreases and approaches the maximum power point (17V). When Rs= 0.9 Ω, curve showed MPP maximum voltage point.

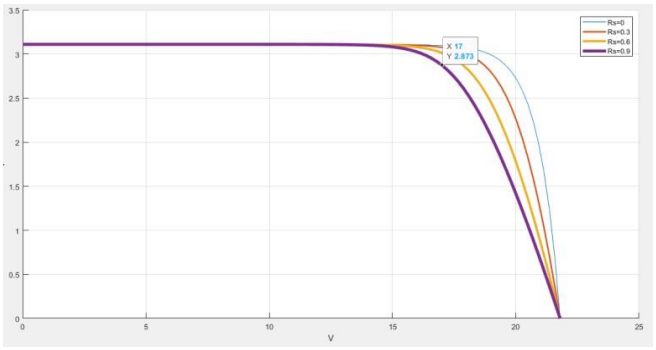

Figure 12 IV characteristics without Rp

Figure 13 shows the PV characteristics in Rs model without considering shunt resistance. As series resistance increases, maximum power point decreases and approaches the maximum power point (49 W). When Rs= 0.9 Ω, curve showed MPP maximum power at 49W. Rp was found to be 185 Ω after substituting Rs in (17).

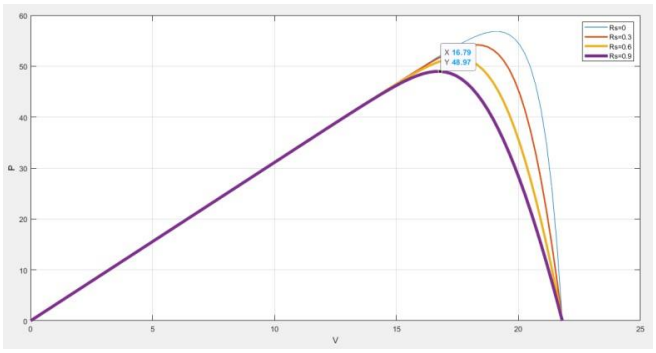

Figure 13 PV characteristics without Rp

Figure 14 represents IV characteristics for the PV model using series and parallel resistances at STC. MPP and maximum current were achieved at 17 V and that verified our model. Imp was 2.85 at 17.004 V (Accurate voltage and current at 17 V could not be measured due to the step size of the cursor in Matlab).

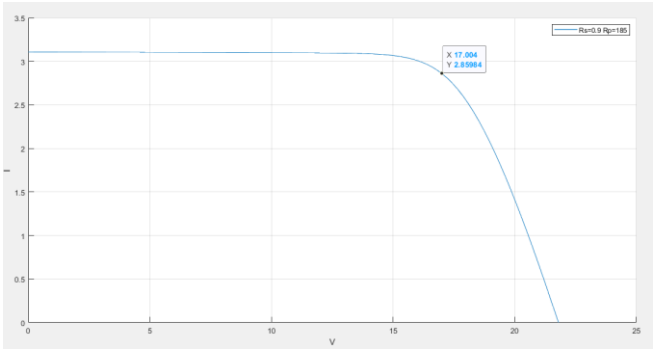

Figure 14 IV characteristics with series and parallel resistances

Figure 15 represents PV characteristics for the PV model using series and parallel resistances at STC. MPP and maximum current were achieved at 17 V and that verified our model. Pmp was 48.774 A at 16.7 V. (Accurate power and current at 17 V could not be measured due to the step size of the cursor in Matlab).

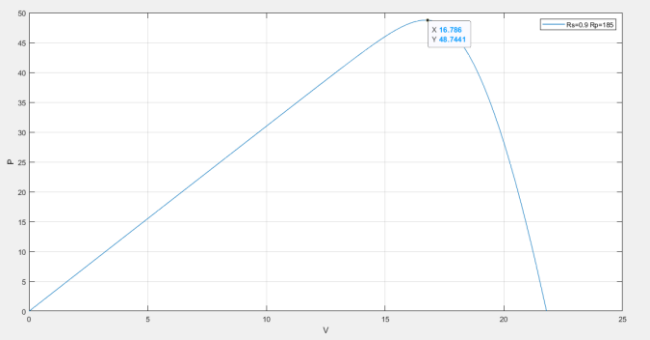

Figure 15 PV characteristics with series and parallel resistances

Figures 16 and 17 show IV and PV characteristics at irradiance of 1000 W/m2 but different temperatures. At a higher temperature, the open circuit voltage decreases to 16.25 V at 60^{0}C. The phenomenon has quite a large impact and it decreases the output power to 34 was temperature increases from 25^{0}C to 60^{0}C.

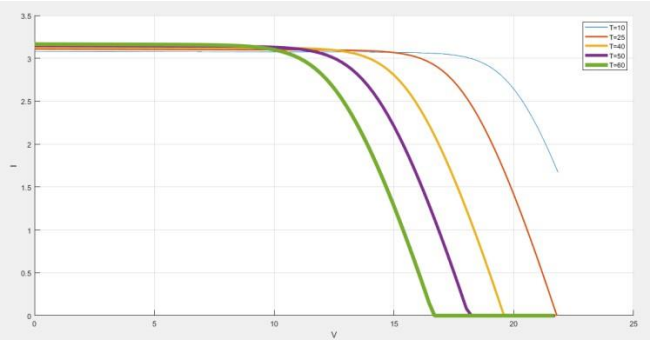

Figure 16 IV characteristics at G=1000 W/m^2 different temperatures

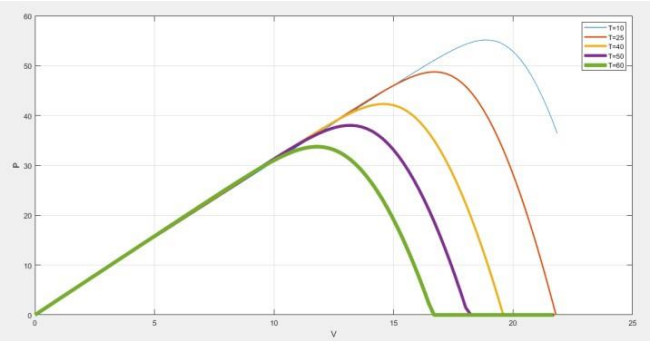

Figure 17 PV characteristics at G=1000 W/m^2 different temperatures

Figures 18 and 19 show IV and PV characteristics at temperature of 25 ^{0}C but different irradiances. At a lower irradiation, the short-circuit current decreases approximately linearly with irradiation It reaches 0.6A at irradiance of 200 W/m^2. The open circuit voltage does notdecrease as much until a very low irradiation. However, it is much more affected by the temperature of the PV-cell.

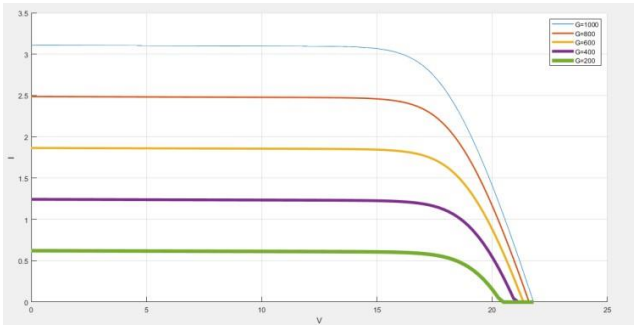

Figure 18 IV characteristics at T=25^{0}C different irradiances

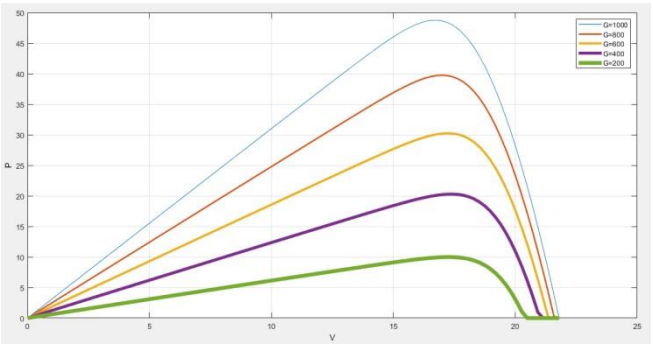

Figure 19 PV characteristics at T=25^{0}C different irradiances

The current is directly proportional to the irradiance while the voltage increases rapidly with increasing irradiance. However, after a specific irradiance, the voltage will be constant regardless of increasing irradiance.

Figure 20 shows the output current pf the PV system before control. Current changes proportionally with changing irradiance. When irradiance is zero, no output current from PV is generated. When irradiance started increasing gradually, this current increases to reach a maximum value of 120 A. We have 40 parallel connected panels and each one has output current at maximum power point 2.88A.

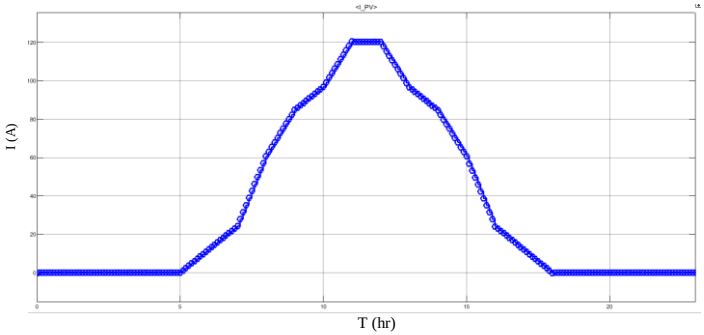

Figure 20 PV Output Current

Figure 21 shows the output voltage of the PV system before control. The voltage is about 151 V when irradiance is zero. At maximum irradiance, the voltage reaches 153.45 V Irradiance effect on this voltage is weak compared to the effect on the current. This verified the PV model discussed in chapter 3. We have 10 series connected panels and each one has the output voltage at maximum power point of 17 V.

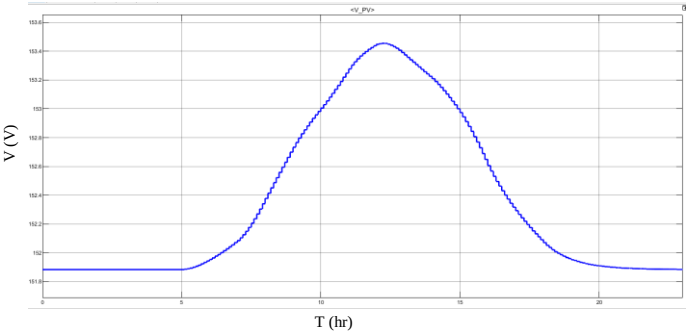

Figure 21 PV Output Voltage

4.2 Results of the PV Model Control System

Figure 22 shows the output voltage of the PV system, where the output voltage at the DC bus increases to reach 437 V. Then it decreases to a constant value, for the rest of the day, at 300 V, which the DC bus voltage required.

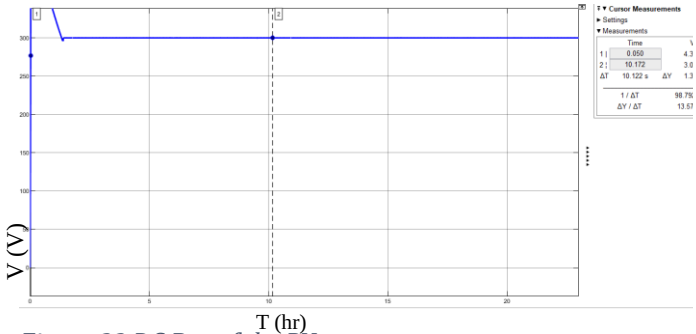

Figure 22 DC Bus of the PV system

4.3 BATTERY SYSTEM OUTPUT

Figure 23a shows the state of charge of the battery system, when no output power generated from PV system, battery will discharge to supply the load to value of 99.999% since simulation time is 23 seconds since Matlab takes long time to simulate a 24 hours system.

Battery will charge when the PV started suppling current and voltage, when the state of charge reaches 100% it remains constant until PV can not supply the demand, then the battery discharged again.

Figure 23 b shows the output current of BESS. During discharge the current is positive, while charging the current is negative it reaches -120 A which is the same as the PV system but with opposite polarity.

Figure 23 c shows the output voltage of the battery, it is the same output voltage of the PV.

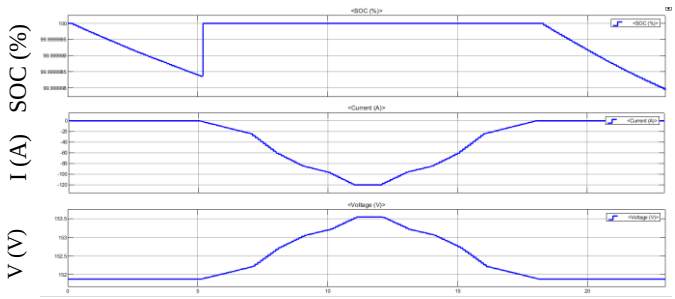

Figure 23: SOC, Current and Voltage of battery system

4.4 Battery System Control

The voltage at the DC bus of the battery reaches a constant value of 130 V after few milliseconds for the rest of the day as shown in Figure 24.

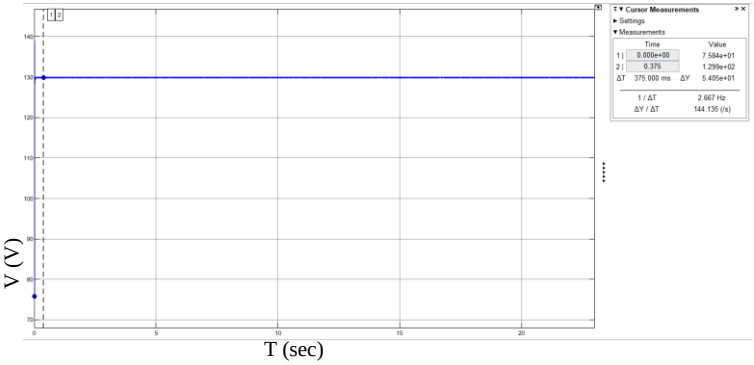

Figure 24 DC Bus of battery

5. CONCLUSION

The presented work calculated the exact series and shunt resistance of a PV model. It is implemented under MATLAB/Simulink environment; the most used software by researchers and engineers. Maximum Power Point (MPPT) parameters (current, voltage and power) have been taken from the datasheet and I(V) and P(V) characteristics curves were plotted at different resistanes until MPP was reaches. Then, relation between series and shunt resistances were used to calculate the shunt resistance.

It is important to compute R_S, even if it is given by a manufacturer because the experimental Maximum Power Point does not match with the computed one. Only one pair satisfies the condition of matching the modeled and the experimental peak power. So, R_s is iteratively increased until satisfying the condition. The proposed R_p model gave (R_s = 0.9 Ω, R_p = 185 Ω).

A boost converter was used to control PV system. This Boost converter was controlled with MPPT (incremental conductance)used for control. Output of the MPPT is the DC voltage reference subtracted from the Duty cycle and then used to generate pulses of the Pulse Width Modulation.

The output voltage at the DC bus increases to reach 437 V, then decreases to constant value, for the rest of the day, of 300 V which is the DC bus voltage required.

Panasonic Lithium-Ion CGR18650AF Lithium Ion Battery is used. Nominal Voltage and capacity were taken from datasheet of a single battery. 36 batteries are connected in series and 125 batteries are connected in parallel,

A bidirectional Boost-Buck Converter was used to control the discharging and charging processes of the Battery System. Boost part controls the discharging process and the Buck part controls the discharging process.

Voltage at the DC bus of the battery increases from 75V to reach constant value of 130 V after few milliseconds for the rest of the day.

II. REFERENCES

[1] WALKER, G. Evaluating MPPT Converter Topologies using a Matlab PV Model.University of Queensland. Australia.

[2] S. Ma Lu "Modelling, Control and Simulation of a Microgrid based on PV System,Battery System and VSC" January 2018.

[3] H. Bellia a,*, R. Youcef b, M. Fatima b"A detailed modeling of photovoltaic module using MATLAB" National Research Institute of Astronomy and Geophysics NRIAG Journal of Astronomy and Geophysics April 2014

[4] Dabra, V. Paliwal, K. K. Sharma, P., Kumar, N.(2017) Optimization of photovoltaic power system: A comparative study. Protection and control of Modern Power Systems 2 (1), 3.

[5] Kumari, J. S., Babu, A. K. (2012). Design and Analysis of P&O and IP&o MPPT techniquies for photovoltaic system. International Journal of Modern Engineering Research, 2(4), 2147-2180

[6] Xuebing, H.; Minggao, O.; Languang, L. A comparative study of commercial lithium ion battery cycle life in electrical vehicle: Aging mechanism identification. // Journal of Power Sources, 251, (2014), pp. 38-54

[7] Sikkabut, S.; Mungporn, P.; Ekkaravarodome, C.; Bizon, N.; Tricoli, P.; Nahid-Mobarakeh, B.; Pierfederici, S.; Davat, B.; Thounthong, P. Control of High-Energy High-Power Densities Storage Devices by Li-ion Battery and Supercapacitor for Fuel Cell/Photovoltaic Hybrid Power Plant for Autonomous System Applications. // IEEE Transactions on Industry Applications, 52, 5(2016), pp. 4395-4407.

[8] Sera, D., Teodorescu, R., Hantschel, J. & Knoll, M. (2008). Optimized maximum power point tracker for fast changing environment conditions. In Industrial Electronics, 2008. ISIE 2008. IEEE International Symposium on (pp. 2401-2407). IEEE.

[9] Faruk, A Yazmadi, A, : "Energy Storage Technologiws for Grid Connected and Off Grid Power System Applications Electrical Power and Engery Conference (EPEC), 2012 IEEE, Publication year: 2012 Page:303. 310

[10] Tremblay, O.; Dessaint, L.-A. Experimental Validation of a Battery Dynamic Model for EV Applications. // World Electric Vehicle Journal, 3, (2009), pp. 289-298.

[11] F. Mohammed "MICROGRID MODELLING AND SIMULATION" Espoo March2016

[12] Geurin, Scott, O: Bames, Arthur: Smart Grid Applications for Selected Eneegry Technologies Innovative Smart Grid Technologies (ISGT), 2012 IEEE PES. Publication Year: 2012, Pages: 1-8

[13] Muhammad H. Rashid, "Power Electronics: Circuits, Devices, and Application". THIRD EDITION

[14] Design and simulation of dc Microgrid in belize D. W. Hart, Power electronics. Tata McGraw-Hill Education, 2011.

[15] Masoum, M.A.S.; Dehbonei, H.; Fuchs, E.F. Theoretical and experimental analyses of photovoltaic systems with voltage- and current-based maximum power-point tracking. IEEE Trans. Energy Convers. **2002**, 17, 514–522.

[16] Ram, J.P., Babu, T.S., Rajasekar, N.: 'A comprehensive review on solar PV maximum power point tracking techniques', Renew. Sustain. Energy Rev., 2017, 67, pp. 826–847

[17] Kumar, D., Chatterjee, K.: 'A review of conventional and advanced MPPT algorithms for wind energy systems', Renew. Sustain. Energy Rev., 2016, 55, pp. 957–970

[18] Yamashita, H.; Tamahashi, K.; Michihira, M.; Tsuyoshi, A.; Amako, K.; Park, M. A novel simulation technique of the PV generation system using real weather conditions. In Proceedings of the Power

[19] Conversion Conference, Osaka, Japan, 2–5 April 2002; Volume 2, pp. 839–844.

[20] Messalti, S.; Harrag, A.; Loukriz, A. A new variable step size neural networks {MPPT} controller: Review, simulation and hardware implementation. Renew. Sustain. Energy Rev. 2017, 68, 221– 233.

[21] M. A. Elgendy, B. Zahawi, and D. J. Atkinson, "Assessment of perturb and observe MPPT algorithm implementation techniques for PV pumping applications," IEEE Transactions on Sustainable Energy, vol. 3, no. 1, pp. 21–33, 2012.

[22] H. Malek and Y. Chen, "BICO MPPT: a faster maximum power point tracker and its application for photovoltaic

panels," International Journal of Photoenergy, vol. 2014, Article ID 586503, 9 pages, 2014.

[23] Dabra, V., Paliwal, K. K., Sharma, P., & Kumar, N. (2017). Optimization of photovoltaic power system: A comparative study. Protection and Control of Modern Power Systems, 2(1), 3.

[24] F. Liu, S. Duan, F. Liu, B. Liu, and Y. Kang, —A variable step size INC MPPT method for PV systems,|| IEEE Trans. Ind. Electron., vol. 55, no. 7, pp. 2622–2628, Jul. 2008

[25] K. H. Hussein, I. Muta, T. Hoshino, and M. Osakada, —Maximum photovoltaic power tracking: An algorithm for rapidly changing atmospheric conditions,|| Proc. Inst. Elect. Eng.—Gener, Transmits. Distrib., vol. 142, no. 1, pp. 59–64, Jan. 1995.

[26] B. Liu, S. Duan, F. Liu, and P. Xu, —Analysis and improvement of maximum power point tracking algorithm based on incremental conductance method for photovoltaic array,|| in Proc. IEEE PEDS, 2007, pp. 637–641.

[27] Y.-C. Kuo, T.-J. Liang and J.-F. Chen, —Novel maximumpower-pointtracking controller for photovoltaic energy conversion system,|| IEEE Trans. Ind. Electron, vol. 48, no. 3, pp. 594–601, Jun. 2001.